15TH IEA HEAT PUMP CONFERENCE
MAY 26–29, 2026 | HOFBURG
VIENNA 2026
DECARBONISATION THROUGH INNOVATION

Towards decarbonization of the agro-food sector: application of a solar-assisted drying process in a juice factory

Valeria Palomba[a*], Giovanni Patanè[b], Matteo Ametta[a], Alessio Sapienza[a], Mauro Prestipino[b]

a National Research Council of Italy – Institute for Advanced Energy Technologies (CNR-ITAE), Salita S.Lucia sopra Contesse 5, 98126 Messina, Italy
b Department of Engineering, University of Messina, C.da di Dio, 98158, Messina, Italy

Abstract

The use of heat pumps in industrial processes is gaining wide attention in the last years, since it allows to strongly diversify the resources needed by the industrial sector, representing up to 24% of overall worldwide CO_2 emissions and 37% of primary energy consumption. Aim of the present work is to assess, through a technical and environmental analysis, the replacement of a drying process powered by gas boilers with a solar-assisted heat pump solution. The industrial process targeted is the drying of a wet biomass, which represents the side product from the juice production. As for the case of citrus peel residues, the dried biomass can be used for animal feeding, pectin or other molecules extraction, and also as fuel for bioenergy systems. Currently, drying is only achieved through gas boilers. The alternative solutions proposed to reduce biomass humidity down to less than 15% is a solar-assisted heat pump process: a high-temperature heat pump, using a low-GWP refrigerant, uses solar heat as the low-temperature source and provides hot air for biomass drying. Electricity for heat pump operation is also supplied by solar energy through PV panels. Starting from real data of the juice factory and experimental data from heat pump testing available in the literature, a TRNSYS model was realised. A sensitivity analysis was carried out, assessing the optimal ratio of solar/PV panels for operation of the heat pump, as well as the optimal sizing of the heat pump to reduce the cost of energy to run the entire drying process. The results indicated that the ratios of 1:1 of solar to heat pump powers is the most suitable one. The average heat pump COP under the examined conditions is 2.9 to 3.2, which allows greater exploitation of the primary energy if compared to the efficiency of gas boilers.

Keywords: TRNSYS; High Temperature Heat pumps; Industrial decarbonization

1. Introduction

Solar Heat for Industrial Processes (SHIP) is gaining wide attention in the last years, since it allows to strongly diversify the resources needed by the industrial sector, representing up 24% of overall worldwide CO_2 emissions and 37% of primary energy consumption [1]. As highlighted in several analyses, the potential for SHIP is relevant for several reasons: solar heat is available everywhere, without need for complex transportation systems, which allows its exploitation both in urban or rural areas also in developing countries [2], the heat needed in several industrial processes is below 300°C, which is fully compatible with the temperature levels from solar collectors [3] and it allows reducing the coal or natural gas dependency of the industrial sector in several countries [4,5]. So far, SHIP is mainly linked to the use of concentrated solar collectors [6–8], which are however of complex installation and maintenance and are mostly suitable as sources for power cycles [9]. For all the processes that require low-temperature heat (<150°C), untapped potential for non-concentrated solar collectors exists [3,10]. One of the most interesting applications for solar heat is the use in solar dryers [11], for which several layouts or solar-assisted dryers integrated with thermal storage and electric boilers or heat pumps have been proposed in recent years. Moreover, agro-food industries are energyintensive and therefore the replacement of primary energy resources within them is of paramount importance [12]. Starting from this context, in the present paper a solar-assisted drying process is proposed for the integration in a juice factory. The dryer is used for the wet biomass that represents the fuel for a CHP-gasification system, that in turns produces heat and power for the industry, thus increasing the circularity of the industrial process [13].

2. System Description

The flow diagram for the industrial process targeted is discussed in [14]: the wet biomass is dried in a furnace to reduce its humidity and use it in a biomass-based gasifier.

The alternative solutions proposed in the current study are shown in Figure 1. The heat needed for the biomass drying to reduce its humidity down to less than 15% can be supplied either by solar collectors entirely or by integrating the solar collectors and a high temperature water/water heat pump, whose heat source can be represented by low-grade heat coming from the industrial processes itself (e.g from condensate of the gas boilers). The high temperature heat pump is driven by PV collectors on the roof of the industrial building.

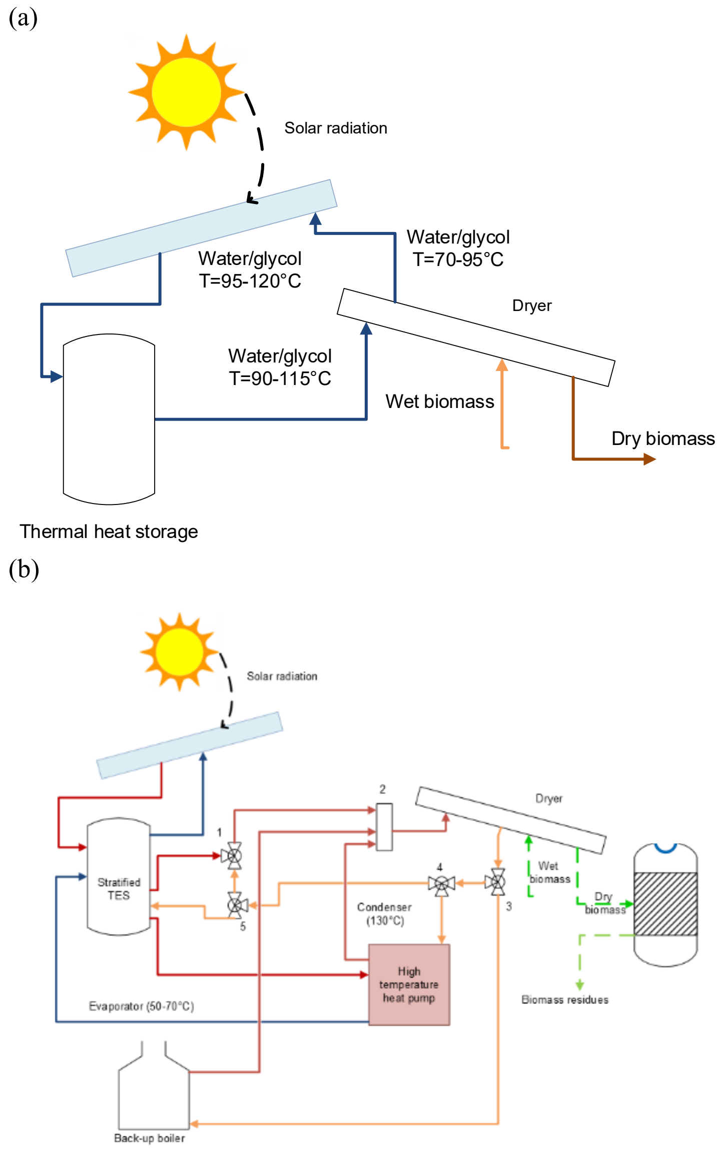

Figure 1: the proposed layout for the solar-assisted dryers: (a) biomass dried using only solar thermal collectors, (b) use of a solar-assisted heat pump.

The proposed system layout is shown in detail in Figure 2. The system is powered by two main sources: PV panels and solar thermal collectors. The PV panels fed energy to the heat pump and the auxiliaries (blowers, pumps), whereas the solar thermal collectors' field is connected to a sensible heat storage (water/glycol) This is connected to both an air-water heat exchanger (HEX), for providing the heat to the dryer, and to the heat pump, to work as the evaporation source for it, according to the logics discussed in the following sections.

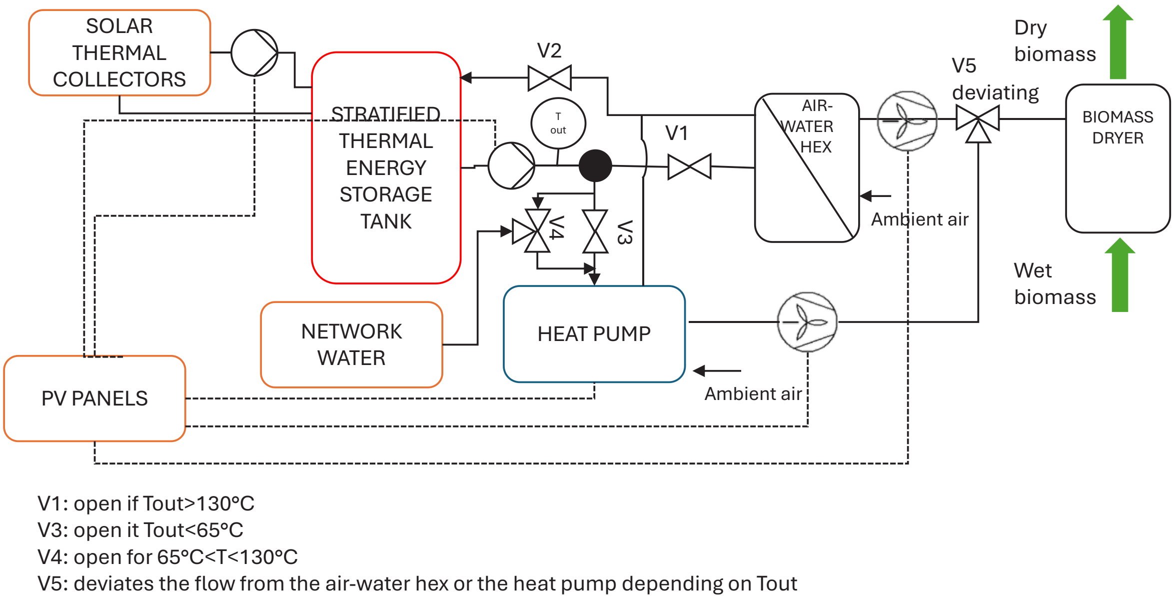

Figure 2: detailed layout of the simulated system.

The high temperature air-water heat pump used for the simulations is the one described in [15], which make use of R1233zd as refrigerant and can work with condenser temperatures between 110°C and 145°C and evaporator temperatures of 40-65°C. The selection of the specific heat pump was done considering that, to the authors' best knowledge, there are no commercial heat pump in the desired capacity and temperature range. Among the work literatures, the heat pump selected has the highest efficiency in the target operating conditions. The schematic of the heat pump is shown in Figure 3 .In addition to condenser, evaporator, compressor and expansion valve, the selected heat pump makes use of an economizer. The economizer plays a dual role in the cycle. First, it increases the degree of subcooling of the refrigerant exiting the condenser. Second, it raises the enthalpy of the refrigerant used for vapor injection, which helps improve the mass flow rate of the injected vapor and therefore increases the overall efficiency of the heat pump. This is especially important considering the high temperature lift at which the heat pump operates.

During operation, the compressor discharges high-pressure, high-temperature vapor, which enters the condenser and is transformed into liquid. This liquid refrigerant then passes to the economizer, where additional subcooling is carried out. After leaving the economizer, the refrigerant divides into two separate flow paths. The primary stream moves through the expansion valve and into the evaporator. There, it vaporizes while absorbing heat, producing a low-pressure, low-temperature vapor that returns to the compressor inlet, where it is compressed again and raised to a higher pressure and temperature. The secondary stream follows the vapor-injection circuit. It first expands through the vapor-injection expansion valve, which reduces both its temperature and pressure, before entering the economizer. Inside the economizer, this auxiliary stream exchanges heat with the subcooled liquid from the condenser. After gaining heat and increasing its enthalpy, this vapor is injected into the compressor's compression chamber to enhance the overall performance of the system. A temperature difference of 5 K between primary and secondary side of the heat exchangers were considered during simulation.

The heating capacity and COP as a function of operating temperatures are graphically reported in Figure 4 .

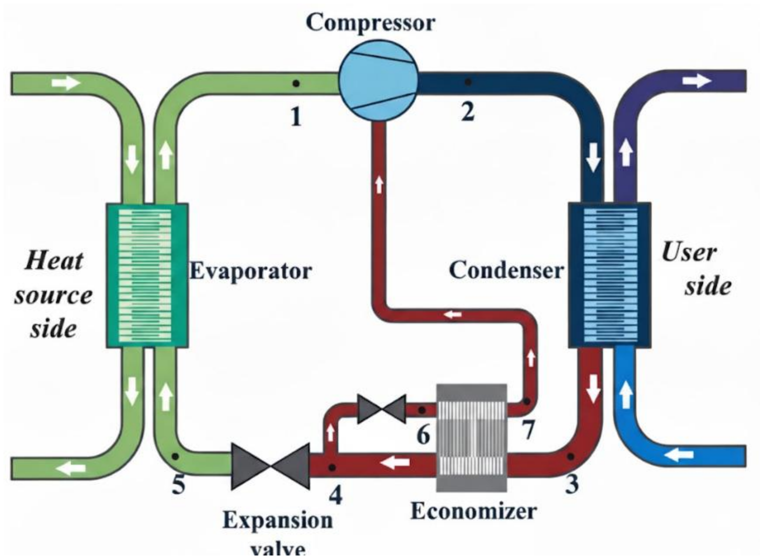

Figure 3: schematic layout of the high temperature heat pump simulated.

(a) (b)

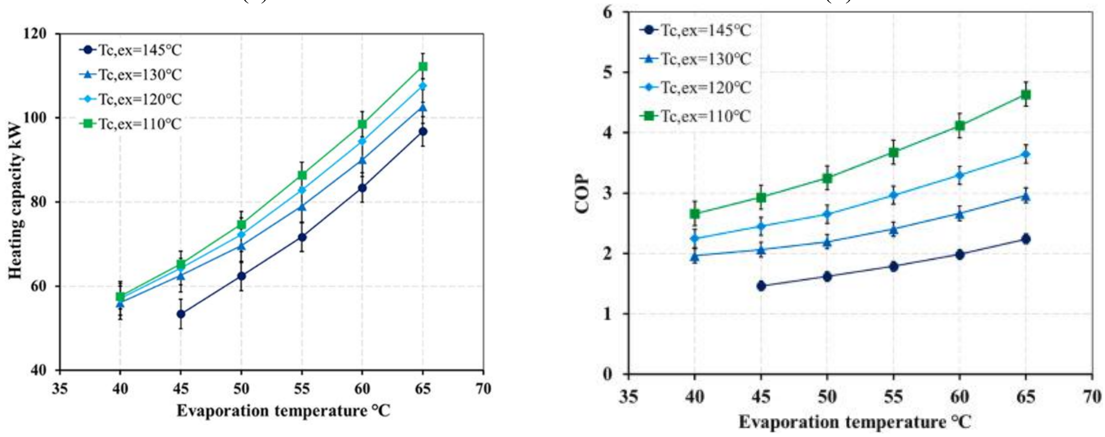

Figure 4: thermal capacity of the heat pump (a) and COP (b) as a function of evaporation temperature for the simulated heat pump. Data from [15]

3. Methodology

The model of the system was realized in TRNSYS18 simulation software. It consists of three main sections:

- PV section, which includes the PV panels, inverter with MPPT function and weather data from Messina.
- The tank subsystem, which includes the solar thermal collector type (type 539) with variable speed pump, and the tank (type 534). The pump speed for the solar thermal collector is regulated in order to keep the desired average temperature (120°C) inside the storage tank. All the hydraulic circuits simulated make use water/30% glycol mixture, to be able to work at temperatures above 100°C. The efficiency of the solar thermal collector according to type 534 is expressed as:

$$\eta = a_0 - a_1 \times \frac{(T-T_{amb})}{G} - a_2 \times \frac{(T-T_{amb})^2}{G} \qquad (1)$$

where T is the temperature of the fluid in the solar collectors, T_{amb} is the ambient temperature, G is the irradiance and a0,a1 and a2 are coefficients provided by the producer.

- The heat pump subsystem. As mentioned before, the heat pump is simulated using performance maps that use the condensation and evaporation temperatures as input variables and gives, as output, the heating capacity and COP (and therefore electricity consumption). Moreover, this subsystem includes the heat source and user side connection. One the user side, there is a thermal regulation system that works as follows – and is reported in Figure 2 as well:

- If the water in the thermal tank is equal or higher than 130°C, then it is directly sent to the dryer;
- If the water from the storage tank is between 65°C and 130:C, it is mixed with network water and used as heat source for the heat pump. The outlet from the heat pump is then sent to the dryer. It can also be recovered for low-temperature loads in the same industrial site.
- If the water from the storage tank is below 65°C it is directly sent to the heat pump as heat source.

The simulations were run for an entire year, considering three cases:

- Rooftop of the building (3500 m^2) entirely covered with 30% solar PV + 70% solar thermal collectors. This case will be called 30/70 in the future discussions;
- Rooftop of the building (3500 m^2) covered with 50% solar PV + 50% solar thermal collectors. This case will be called 50/50 in the future discussions;
- Rooftop of the building (3500 m^2) entirely covered with solar PV. This case will be called 0/100 in the future discussions.

4. Results

The time-based load for the biomass drier is reported in Figure 5, which highlights that the biomass dryer thermal load is highly variable (approximately 200–700 kW on an hourly basis), with a seasonal reduction during July–August due to reduced production activity (holiday period). This variability is important because it impacts both the instantaneous condenser-side heat requirement and the operating duty cycle of the heat pump subsystem. In particular, load reductions during summer coincide with higher solar availability, which enables higher solar fractions and reduced grid reliance. Conversely, in winter months, the dryer load remains significant while solar availability decreases, thus increasing the probability of heat pump operation at lower evaporator inlet temperatures and higher electricity import from the grid.
The average COP of the high temperature heat pump throughout the year for the three examined cases is reported in Figure 6. The trends in Figure 7 can be explained by the evaporator-side inlet temperature delivered by the thermal storage tank. In the 30/70 and 50/50 scenarios, solar thermal collectors maintain the tank temperature partially within the 65–130°C interval for a significant portion of the year. In that operating range, the tank can provide preheated source water to the heat pump, increasing the evaporator temperature and reducing the temperature lift across the compressor. This directly leads to higher COP values (typically 3.5–5.0). In contrast, in the 0/100 scenario the evaporator source temperature remains close to the minimum allowable value (≈65°C), since no solar thermal contribution is available. Consequently, the temperature lift remains higher and the COP stabilizes around 2.7, representing a conservative (worst-case) operating condition for the heat pump. These results confirm that solar thermal integration increases the thermodynamic efficiency of the heat pump, even though it may reduce PV electricity generation area.
Figure 7 reports the hourly net electricity exchanged with the grid, computed as the difference between PV production and the combined consumption of the heat pump and auxiliary components (pumps, blowers, and circulation). Positive values correspond to PV surplus exported to the grid, while negative values indicate the fraction of electricity that must be imported. Since electrical storage is not included in the present analysis, the reported grid exchange represents the instantaneous balance between production and consumption, and therefore provides a measure of the system's ability to achieve direct solar self-consumption in each rooftop scenario. The comparison between March and June 8 highlights the strong seasonal dependence of electrified drying systems. In June, PV production is high and the thermal load is reduced, resulting in frequent PV surplus conditions (positive values) and a reduced need for grid import, particularly for the 0/100 scenario. In March, the mismatch between demand and solar availability is larger, increasing the frequency and magnitude of negative values. This behavior confirms that the rooftop partition strongly affects not only annual energy values but also the operational stability and grid dependency during transitional and winter periods.
It is however worth noting that the 0/100 case does not represent the most stable operating condition for the system, since no heat storage is foreseen. Should a similar layout be chosen, a thermal energy storage tank on the user side of the heat pump should be added, together with a proper energy management system that should charge/discharge the thermal energy storage in a smart way according to demand/response considerations from the electric network, which would add extra costs and complexity in system management.
Finally, the overall energy consumption and reduction in CO2 emissions for the three cases – compared to the baseline – was calculated.

In the current configuration of the citrus-processing plant, citrus-pulp drying is performed in a methane-fired furnace, whose thermal efficiency is reported by the company to be approximately 84%. Using the thermal loads required by the dryer, the annual energy demand was obtained by summing the hourly outputs generated by the TRNSYS model, yielding an annual useful thermal energy requirement of about 19 TWh. Considering the lower heating value of methane, the overall consumption is $1.8*10^6$ m^3/y. According to the emission factors[16], non-renewable methane combustion releases around 0.202 tCO_2/MWh, leading to annual CO_2 emissions of roughly 3,878 tCO_2 for the existing system.
For the proposed layout, the annual electricity consumption drawn from the grid is:

- 70/30 scenario: $2.33 \times 10^6 kWh/y$
- 50/50 scenario: $2.27 \times 10^6 kWh/y$
- 0/100 scenario: $1{,}13 \times 10^6 kWh/y$

Using the national Italian electricity emission factor of 0.284 tCO_2/MWh, the corresponding CO_2 emissions are 662 tCO_2, 608 tCO_2, and 321 tCO_2, respectively. Compared with the baseline system, these scenarios yield annual emission reductions of 82.9%, 84.3%, and 91.7%, demonstrating the significant environmental benefits associated with the proposed configuration.

(a)

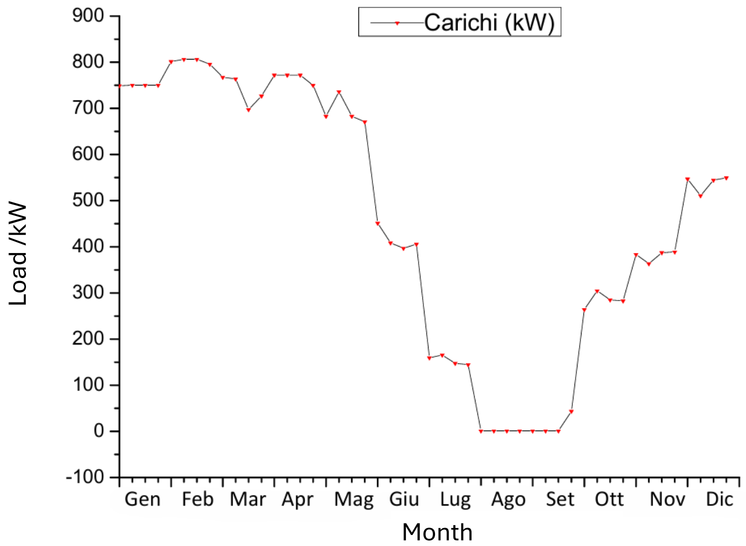

(b)

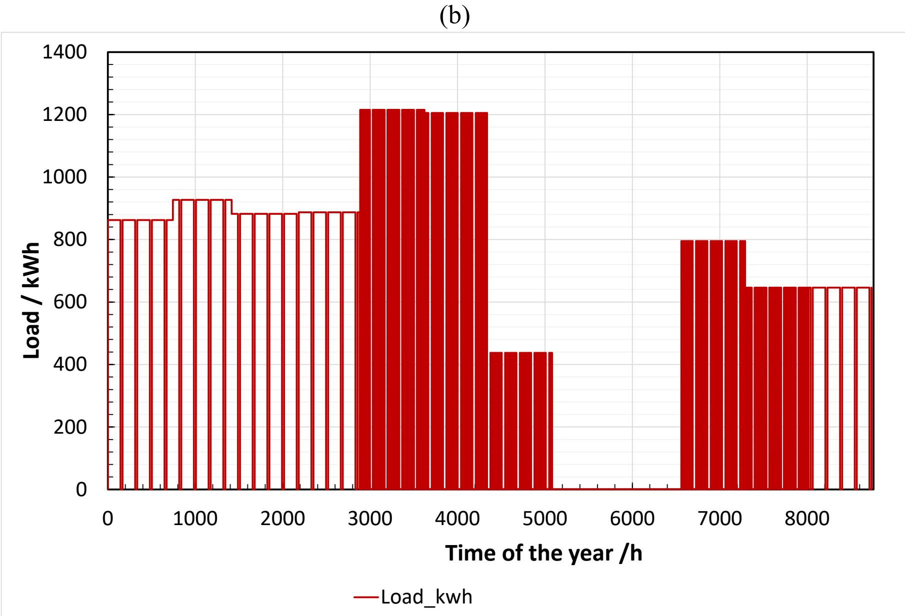

Figure 5: biomass dryer loads. (a) average monthly load; (b) hourly values

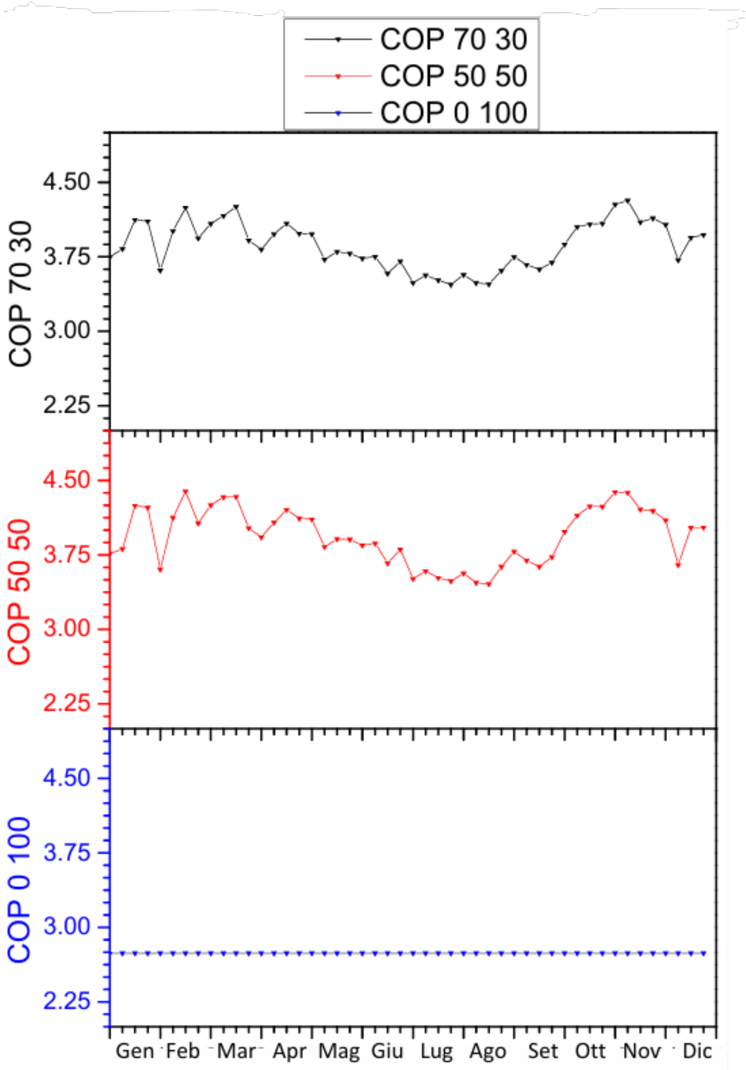

Figure 6: average COP of the high temperature heat pump in the three cases examined.

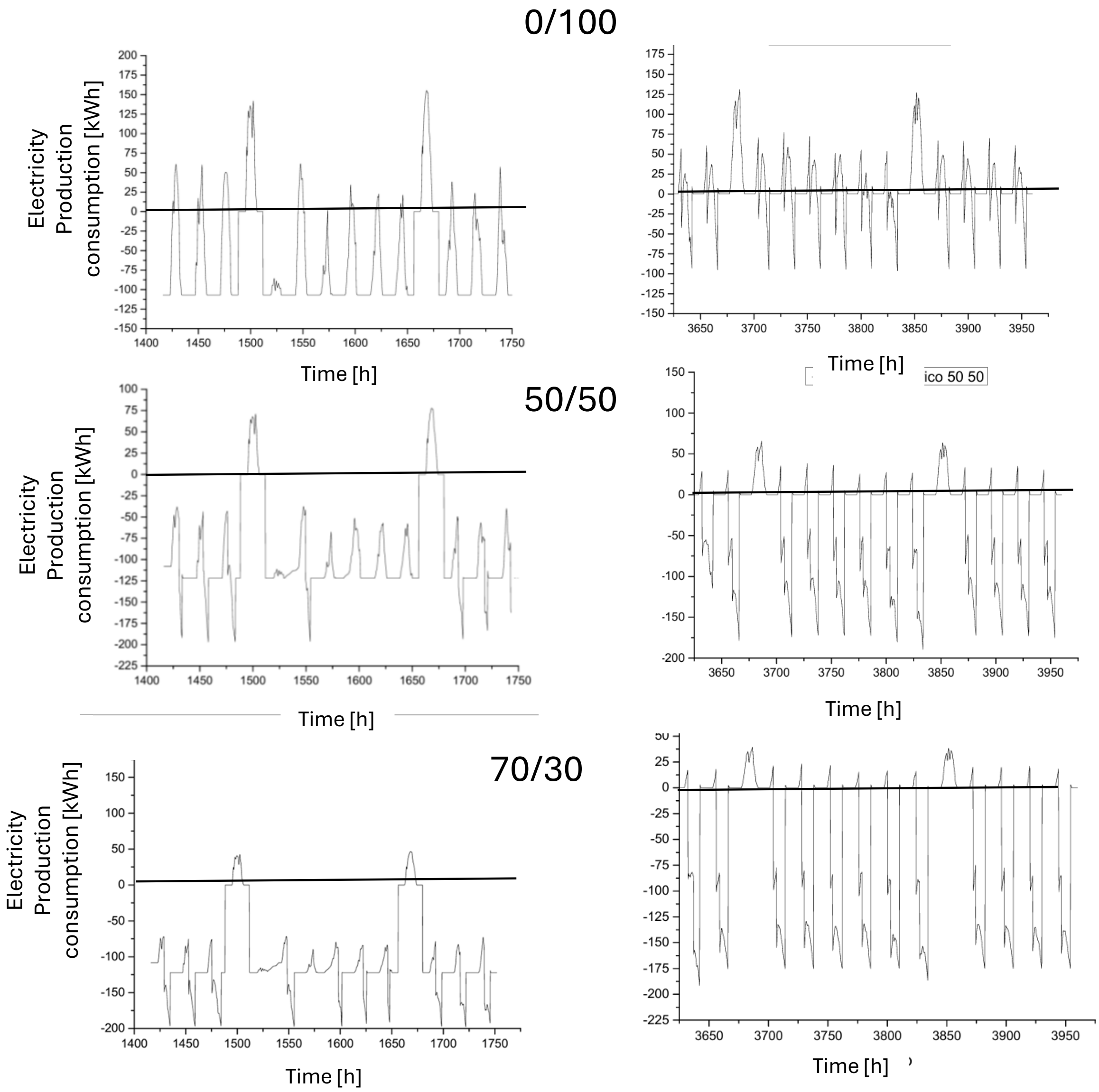

Figure 7: electricity produced and consumed for the examined cases in March (left) and June (right).

5. Conclusions

This study developed and assessed an alternative drying system for citrus by-products, starting from the existing configuration of a Sicilian processing facility and proposing a hybrid renewable layout aimed at improving energy efficiency and reducing carbon emissions. The current plant relies solely on a natural-gas-fired dryer, whereas the proposed solution integrates photovoltaic and solar-thermal collectors, thermal storage, a water–air heat exchanger, and a high-temperature heat pump. Three allocation scenarios for the available rooftop area were simulated using TRNSYS, varying the fraction dedicated to solar-thermal collectors (70%, 50%, and 0%) while assigning the remaining surface to photovoltaics. The simulation results show that dedicating the entire rooftop area to photovoltaic modules (0/100 scenario) offers the highest degree of electrification and the greatest reduction in grid consumption. Relative to the current gas-fired system, the 70/30 and 50/50 configurations achieve CO_2-emission reductions of 82.9% and 84.3%, respectively, while the 0/100 case reaches a reduction of 91.7%, confirming it as the most effective option for decarbonizing and improving the efficiency of the drying process.

Future work may involve exploring additional rooftop-area partitions, extending the seasonal analysis across the full year, evaluating the integration of electrical storage to increase self-consumption, assessing the inclusion of a safety chiller to ensure optimal operating conditions, and employing more detailed TRNSYS components to enhance model accuracy.Overall, the results highlight the strong potential of hybrid renewable systems and process electrification to support the decarbonization of the agri-food sector, while simultaneously improving energy efficiency and contributing to the environmental and economic sustainability of industrial operations.

Acknowledgements

We acknowledge financial support under the National Recovery and Resilience Plan (NRRP), Mission 4, Com-ponent 2, Investment 1.1, Call for tender No. 104 published on 2.2.2022 by the Italian Ministry of University and Research (MUR), funded by the European Union – NextGenerationEU– Project Title REHP-4-TUNE: Renewable Electric High-tem-perature Heat Pumps For Thermal Users in Neutral CO2 Environments – CUPmaster J53D23002060006 – CUP B53D23005860006, Grant Assignment Decree No. 961 adopted on the 30th of June 2023 by the Italian Ministry of Ministry of University and Research (MUR).

References

[1] Schoeneberger CA, McMillan CA, Kurup P, Akar S, Margolis R, Masanet E. Solar for industrial process heat: A review of technologies, analysis approaches, and potential applications in the United States. Energy 2020;206:118083. https://doi.org/10.1016/J.ENERGY.2020.118083.

[2] Farjana SH, Huda N, Mahmud MAP, Saidur R. Solar process heat in industrial systems – A global review. Renewable and Sustainable Energy Reviews 2018;82:2270–86. https://doi.org/10.1016/J.RSER.2017.08.065.

[3] Lauterbach C, Schmitt B, Jordan U, Vajen K. The potential of solar heat for industrial processes in Germany. Renewable and Sustainable Energy Reviews 2012;16:5121–30. https://doi.org/10.1016/j.rser.2012.04.032.

[4] jia T, Huang J, Li R, He P, Dai Y. Status and prospect of solar heat for industrial processes in China. Renewable and Sustainable Energy Reviews 2018;90:475–89. https://doi.org/10.1016/J.RSER.2018.03.077.

[5] McMillan C, Xi W, Zhang J, Masanet E, Kurup P, Schoeneberger C, et al. Evaluating the economic parity of solar for industrial process heat. Solar Energy Advances 2021;1:100011. https://doi.org/10.1016/J.SEJA.2021.100011.

[6] Renewable Energy Agency I. IEA-ETSAP and IRENA Solar Heat for Industrial Processes ENERGY TECHNOLOGY SYSTEMS ANALYSIS PROGRAMME. n.d.

[7] von Storch H, Roeb M, Stadler H, Sattler C, Bardow A, Hoffschmidt B. On the assessment of renewable industrial processes: Case study for solar co-production of methanol and power. Appl Energy 2016;183:121–32. https://doi.org/10.1016/J.APENERGY.2016.08.141.

[8] jia T, Huang J, Li R, He P, Dai Y. Status and prospect of solar heat for industrial processes in China. Renewable and Sustainable Energy Reviews 2018;90:475–89. https://doi.org/10.1016/J.RSER.2018.03.077.

[9] Crespi F, Sánchez D, Rodríguez JM, Gavagnin G. A thermo-economic methodology to select sCO2 power cycles for CSP applications. Renew Energy 2020;147:2905–12. https://doi.org/10.1016/j.renene.2018.08.023.

[10] Miró L, Gasia J, Cabeza LF. Thermal energy storage (TES) for industrial waste heat (IWH) recovery: A review. Appl Energy 2016;179:284–301. https://doi.org/10.1016/j.apenergy.2016.06.147.

[11] Nukulwar MR, Tungikar VB. Recent development of the solar dryer integrated with thermal energy storage and auxiliary units. Thermal Science and Engineering Progress 2022;29:101192. https://doi.org/10.1016/J.TSEP.2021.101192.

[12] Zhang XR. Study on the solar energy heat pump space heating system in the agricultural and pastoral areas in inner Mongolia. Lecture Notes in Energy, vol. 33, Springer Verlag; 2017, p. 29–45. https://doi.org/10.1007/978-3-319-26950-4_2.

[13] Galvagno A, Prestipino M, Zafarana G, Chiodo V. Analysis of an Integrated Agro-waste Gasification and 120kW SOFC CHP System: Modeling and Experimental Investigation. Energy Procedia 2016;101:528–35. https://doi.org/10.1016/j.egypro.2016.11.067.

[14] Galvagno A, Prestipino M, Maisano S, Urbani F, Chiodo V. Integration into a citrus juice factory of air-steam gasification and CHP system: Energy sustainability assessment. Energy Convers Manag

2019;193:74–85. https://doi.org/10.1016/j.enconman.2019.04.067.
[15] Wu D, Wei J, Hu B. Theoretical analysis, experimental research and industrial verification of high temperature heat pump based on R1233zd(E). Energy 2025;319:135175. https://doi.org/10.1016/J.ENERGY.2025.135175.
[16] Emissions Factors 2021 - Data product - IEA n.d. https://www.iea.org/data-and-statistics/data-product/emissions-factors-2021 (accessed November 13, 2025).